



Article

Evaluation and Analysis of Remote Sensing-Based Approach for Salt Marsh Monitoring

David F. Richards IV , Adam M. Milewski *, Steffan Becker, Yonesha Donaldson, Lea J. Davidson, Fabian J. Zowam, Jay Mrazek and Michael Durham

Water Resources & Remote Sensing Laboratory (WRRS), Department of Geology, University of Georgia, 210 Field Street, 306 Geography-Geology Building, Athens, GA 30602, USA; david.richards25@uga.edu (D.F.R.IV); steffanbecker96@gmail.com (S.B.)

* Correspondence: milewski@uga.edu

Abstract: In the United States (US), salt marshes are especially vulnerable to the effects of projected sea level rise, increased storm frequency, and climatic changes. Sentinel-2 data offer the opportunity to observe the land surface at high spatial resolutions (10 m). The Sentinel-2 data, encompassing Cumberland Island National Seashore, Fort Pulaski National Monument, and Canaveral National Seashore, were analyzed to identify temporal changes in salt marsh presence from 2016 to 2020. ENVI-derived unsupervised and supervised classification algorithms were applied to determine the most appropriate procedure to measure distant areas of salt marsh increases and decreases. The Normalized Difference Vegetation Index (NDVI) was applied to describe the varied vegetation biomass spatially. The results from this approach indicate that the ENVI-derived maximum likelihood classification provides a statistical distribution and calculation of the probability (>90%) that the given pixels represented both water and salt marsh environments. The salt marshes captured by the maximum likelihood classification indicated an overall decrease in salt marsh area presence. The NDVI results displayed how the varied vegetation biomass was analogous to the occurrence of salt marsh changes. Areas representing the lowest NDVI values (−0.1 to 0.1) corresponded to bare soil areas where a salt marsh decrease was detected.

Keywords: remote sensing; salt marsh; hydrology; coastal; Sentinel-2; NDVI



Citation: Richards, D.F., IV; Milewski, A.M.; Becker, S.; Donaldson, Y.; Davidson, L.J.; Zowam, F.J.; Mrazek, J.; Durham, M. Evaluation and Analysis of Remote Sensing-Based Approach for Salt Marsh Monitoring. *Remote Sens.* **2024**, *16*, 2. <https://doi.org/10.3390/rs16010002>

Academic Editor: Andy Steven

Received: 17 November 2023

Revised: 15 December 2023

Accepted: 16 December 2023

Published: 19 December 2023



Copyright: © 2023 by the authors. Licensee MDPI, Basel, Switzerland. This article is an open access article distributed under the terms and conditions of the Creative Commons Attribution (CC BY) license (<https://creativecommons.org/licenses/by/4.0/>).

1. Introduction

Coastal salt marshes are some of the most vulnerable and threatened natural ecosystems [1–3]. These ecosystems serve as wetlands in the upper coastal intertidal zone between the upland coastal plain and aquatic brackish waters, helping to control ecosystem function and structure. In this transition zone, salt marshes experience the impacts of alternating high and low tides, causing salt marsh diebacks following extreme precipitation and flooding events [4–6]. As these salt marshes evolve, changes in channelization occur, contributing to the hydrologic dynamic [7,8]. Salt marsh migration alters hydrologic processes, which are part of a multidimensional hydrogeological framework [9,10]. In addition, these events have made salt marshes highly susceptible to geomorphological changes that cause erosional effects and subsidence in response to an increased sea level rise [11]. As the climatic regime effects serve as a prominent factor in altering these ecosystems, increased anthropogenic activity impacts these systems tangentially [12–14]. The South Atlantic salt marshes of the United States (US) are representative of some of the most vulnerable salt marshes globally. Spanning the coasts of North Carolina (NC), South Carolina (SC), Georgia (GA), and Florida (FL), approximately 1 million acres (404,686 hectares (ha)) of salt marshes are threatened by climate change and the human-induced impact that degrades salt marsh environments [15].

Globally, salt marshes are decreasing, with a loss of approximately 25% to 50% of their vegetative cover [16–18]. Over the past 300 years, global salt marshes have declined in

area by 87%, and they have declined 54% since 1900 [19]. A recent study suggested that approximately 561 square miles (1453 square kilometers) of salt marshes have been removed over the past 20 years worldwide [20]. By 2060, the National Oceanic and Atmospheric Administration (NOAA) estimates that 14% to 34% of existing South Atlantic salt marshes could be lost [21]. These studies have shown how vital *Spartina* salt marshes are, and due to their increased vulnerability, proper mitigation is imperative to provide natural coastal resource management. Traditionally, salt marshes have been analyzed through field-based techniques; however, due to limited access to some areas, the use of remote sensing has been implemented [22,23]. Remote sensing techniques offer the opportunity to monitor short- and long-term landscape changes under high spatial resolutions to provide mapping accuracy. Specifically, salt marsh environments have been analyzed using data collected from various satellites to distinctively characterize how they have changed over time [24–28].

The development of salt marsh monitoring has evolved due to the increase in changes to the ecomorphodynamic response due to climate change [29–31]. Coastal salt marshes are experiencing extreme temperatures, changes in storm frequency and intensity, sediment redistribution, changes in nutrient inputs, and the oscillation of high and low tides [32–37]. These processes consequently impact salt marsh growth and resilience as well as the ability to provide the necessary barrier for aquatic life and resources. When this occurs, the geomorphic characterization of these regions is altered, causing changes to the hydrologic/hydrogeologic interface [37–40]. Modeling and field-based techniques have been used and have been shown to be useful in understanding vegetative changes [10,41,42]. Field-based techniques have provided valuable data; however, the collection of data has become more difficult in densely vegetated areas, and as such, the use of remote sensing-based tools has been introduced [10,41,42]. Remote sensing-based salt marsh monitoring has become a catalyst in providing long-term datasets to assess the variability and trends occurring in salt marshes. Through satellite observations, imagery products provide multi-temporal datasets for salt marsh monitoring. Sentinel datasets provide high spatial resolutions with efficient temporal sampling to identify rapid changes [43]. Unmanned aerial vehicles (UAVs) have been used to measure the influence of morphological changes on salt marshes [44]. Furthermore, large-scale computing using Google Earth, a cloud-based platform, has made it easy to access large geospatial datasets in a suitable fashion [45,46]. As current research and monitoring of salt marshes continue to progress, challenges remain. Can coupled-based classification schemes identify small-scale changes? Can validation techniques be implemented to increase accuracy? How can coupled-based classification scheme approaches improve accuracy? As these questions persist, the instituted approach aims to provide solutions to these questions. The ability to use field-based data and manually selected ROIs under supervised classification schemes provides a nuanced approach to better interpret salt marsh changes; thus, the improvement of classification techniques is still needed [47]. Here, we explored methods to identify and quantify how salt marshes are changing along the southeastern coast of the US and how they can provide valuable data for coastal natural resource management.

Field-based and remote sensing techniques are often used, but not always in unison. The integration of both techniques allows for a better understanding of the changes occurring in these ecosystems. In this study, we evaluated and applied a remote sensing-based modeling approach in conjunction with field-based data to determine vegetative cover changes in salt marshes located in the National Park Service (NPS) areas along the US South Atlantic coastline. The vegetative cover changes detailed areas of salt marsh increase and/or decrease between two specified time periods. In addition, we spatially characterized the vegetative biomass by identifying the vegetation density and relative growth. From this analysis, this study outlined the classification algorithms that are most appropriate for mapping salt marshes. Thus, the purpose of this paper was to evaluate the usefulness of the classification schemes, determine the best classification method, and demonstrate classifications representative of the southeast US. This monitoring approach

can be implemented to improve salt marsh management as well as inform natural resource conservation management on how to better protect them.

2. Study Area

The NPS areas along the South Atlantic coastline included in this study were Fort Pulaski National Monument (NM) in Savannah, GA; Cumberland Island National Seashore (NS) in Camden County, GA; and Canaveral National Seashore (NS) in Titusville, FL (Figure 1). Each of these sites was selected due to the high proportion of marsh land in the area. Cumberland Island NS is representative of the largest and southernmost barrier island along the South Atlantic, where the NPS estimates that there are 9341 acres (3780 ha) of salt marsh [48]. At Fort Pulaski NM, the NPS estimates that approximately 90% of the monument is classified as a wetland, including over 4800 acres (1942 ha) of salt marsh [49]. The NPS categorizes Canaveral National Seashore as a barrier island where the salt marshes cover approximately 4400 acres (1781 ha) of the seashore [50].

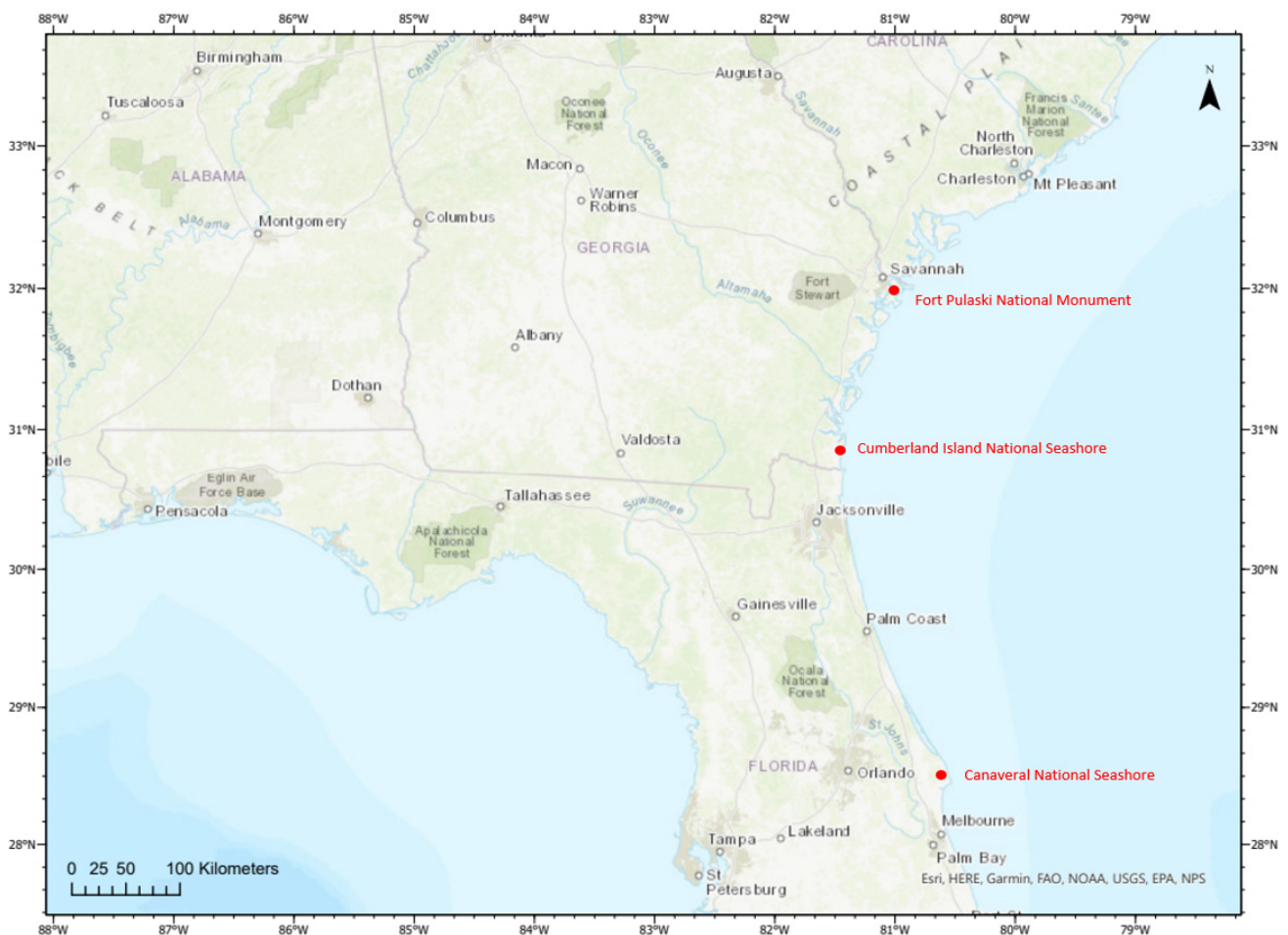


Figure 1. Cumberland Island National Seashore, Canaveral National Seashore, and Fort Pulaski National Monument site locations.

Cumberland Island NS is approximately 36,423 acres (13,526 ha). Of this area, salt marshes occupy approximately 9019 acres (3650 ha), and the dominant vegetative type is *Spartina alterniflora* (smooth cordgrass) [48]. In the marsh areas, this region is mostly comprised of poorly drained soils in tidal marshes and poorly drained soils in shallow depressions [48]. Since Cumberland Island NS is near Fort Pulaski NM, the site's climate and average precipitation are considered the same [48,49,51].

Fort Pulaski NM is approximately 90% wetland, and the majority of the vegetation is *Spartina alterniflora* (smooth cordgrass) [49]. This marsh land represents areas of marshy

soil and a black to bluish-gray heavy silt, and it contains large amounts of shells and decaying organic matter [49]. The climate at this site is hot to humid during the summer (88.0–89.6 °F, 31–32 °C), with mild, brief cold periods (39.3–42.8 °F, 4–6 °C) during the winter [49,51]. Storm fronts of precipitation events usually occur during the winter and spring months, while tropical storms, hurricanes, and thunderstorms occur during the fall and summer months [49,51]. This site receives approximately 1201–1400 mm/year (47.3–55.1 inches/year) of rain [49,51].

Canaveral NS is approximately 58,807 acres (23,798 ha). The vegetative types present in the salt marshes are *Spartina (Juncus)*, mangroves, and saltwort (saltgrass), representing approximately 13% of the area [50]. The climate in this area is semi-tropical to temperate; the summer months are hot and humid (88.0–90.0 °F, 31–32.2 °C), and winter months range in temperature from 30.0 to 70.0 °F (−1 to 21.1 °C) [50,51].

3. Methodology

The approach developed involved the classification of salt marsh presence with a data processing procedure, the calculation of vegetation biomass, and the determination of changes occurring within each site. Sentinel-2 data (2016–2020) were acquired from the United States Geological Survey (USGS) Earth Explorer (Figure 2). Two Sentinel-2 images were acquired for each site: Cumberland Island NS (6 September 2019 and 19 March 2020), Fort Pulaski NM (30 December 2016 and 21 October 2018), and Canaveral NS (20 November 2016 and 31 October 2017). The selected images were selected at different tidal stages. Fort Pulaski NM and Cumberland Island NS were in the tidal stage of 1.8–2.7 m (m), while the Canaveral NS tidal stage was 0.3–0.6 m. To identify the salt marshes present, unsupervised and supervised classification schemes were used to determine each class (Figure 3). The classes were then validated using manual pixel selection and field-based training data collection. To calculate the vegetation biomass, the Normalized Difference Vegetation Index (NDVI) was applied at each site. These results yielded a change analysis identifying the areas of salt marsh increase (%) and decrease (%).

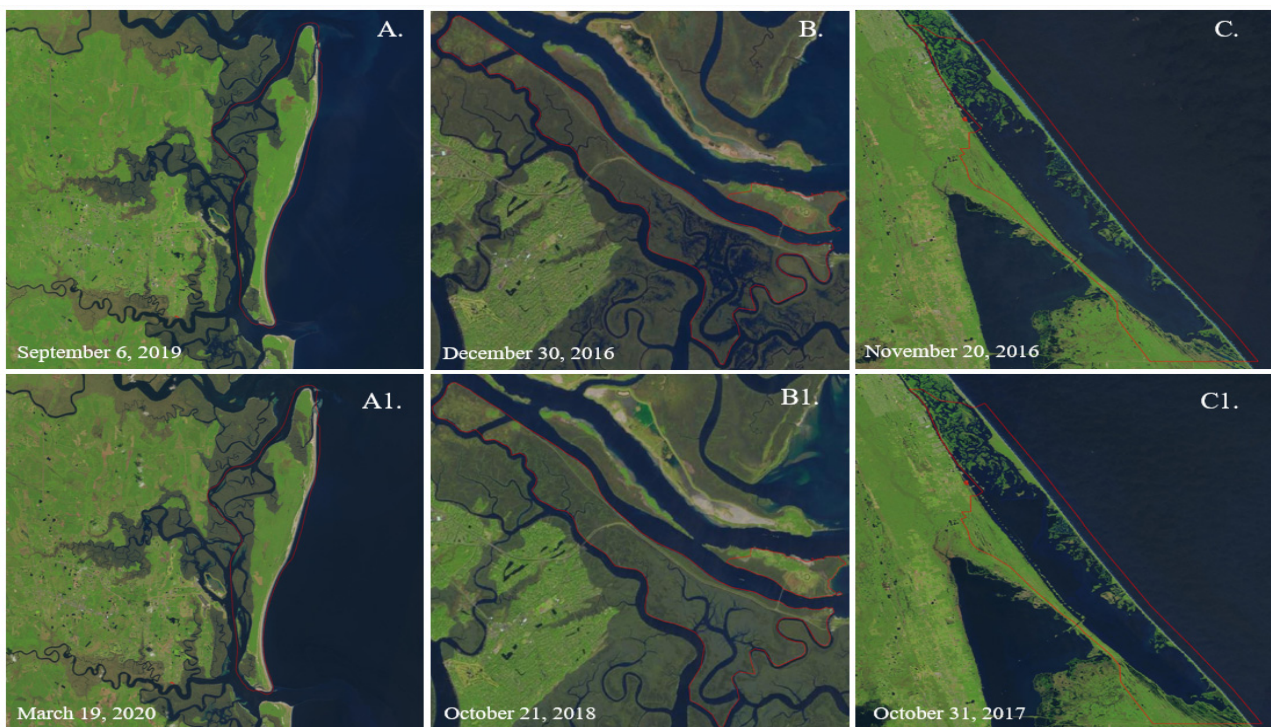


Figure 2. Sentinel-2-derived site locations: Cumberland Island NS (A,A1), Fort Pulaski NM (B,B1), and Canaveral NS (C,C1). Top panel (A–C) represents the initial Sentinel-2 image collected to compare with the bottom panel (A1,B1 and C1.) of the changes that occurred in a different year.

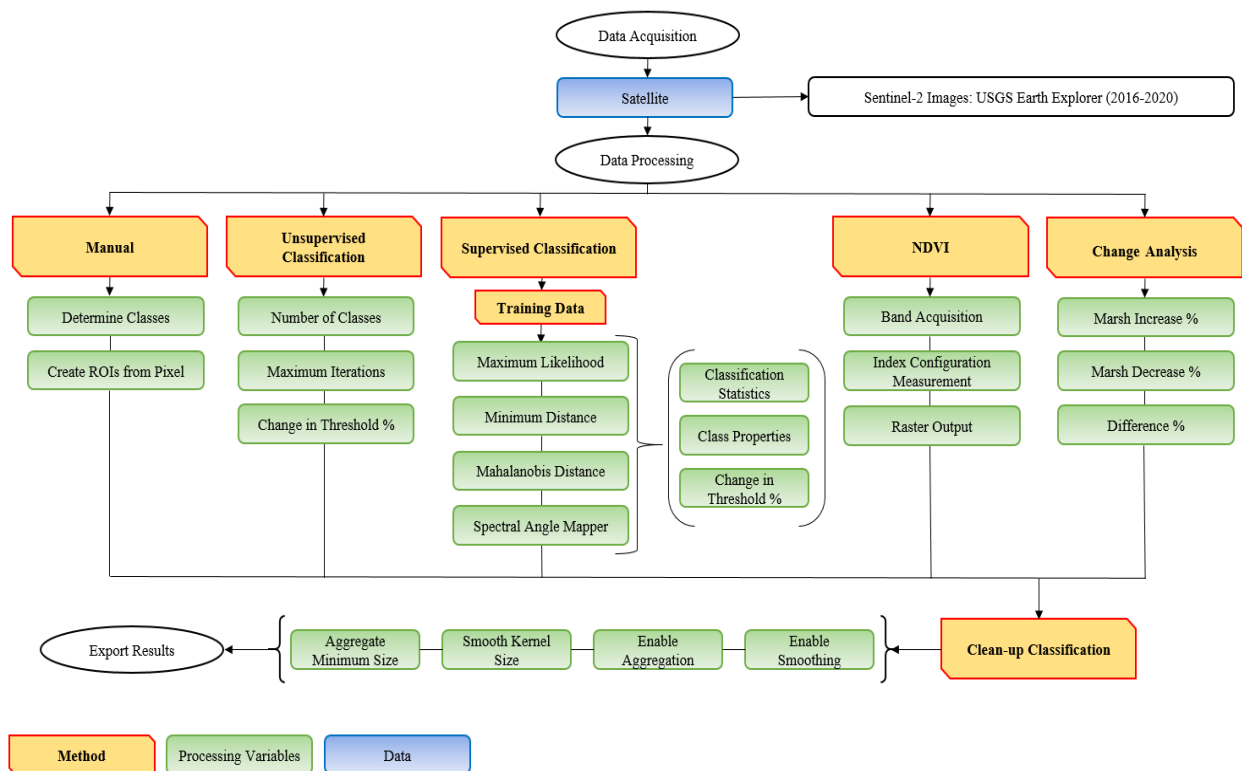


Figure 3. Processing procedure representing data acquisition, data processing, and final output. Each processing method was used to characterize salt marshes spatially and temporally.

3.1. Data Acquisition

Sentinel-2 data (10 m resolution) were collected from 2016 to 2020 at each NPS site. The Sentinel-2 data product was distributed as a Level-1C top-of-atmosphere (TOA) reflectance orthorectification to generate highly accurate geolocated products from the USGS Earth Explorer and the European Space Agency (ESA) [52]. Each Level-1C product is a 100 km × 100 km tile with a UTM/WGS84 (Universal Transverse Mercator/World Geodetic System 1984) projection and datum. The Level-1C product is the result of applying a Digital Elevation Model (DEM) to project the image in cartographic geometry [53]. Radiometric measurements are taken from each pixel and projected in TOA reflectance along with the parameters to transform them into radiances (the formula is below) [53]. Level-1C processing applies radiometric and geometric corrections (including orthorectification and spatial registration). The Level-1C dataset was processed from its true color image. Each data file can be accessed here: <https://sentinels.copernicus.eu> (accessed on 21 July 2023).

The formula conversion for reflectance to radiance is as follows:

$$\text{radiance} = \text{reflectance} * \cos(\text{radians}(\text{SunZenithAngle})) * \text{solar Irradiance} * U(\text{thermal transmittance})/\pi$$

3.2. Data Processing

To perform this analysis, a classification workflow was created in ENVI 5.3-NV5 Geospatial to categorize the pixels in an image into different classes using supervised and unsupervised classification schemes. The unsupervised classification schemes (K-means and IsoData) were performed using no training data, while the supervised classification schemes (maximum likelihood, minimum distance, Mahalanobis distance, and spectral angle mapper) trained the algorithm using manual data input from existing region-of-interest (ROI) and field-based data. These classification schemes have been used in coastal vegetative environments to better predict and understand the changes that are occurring [54–56]. Additionally, the NDVI was used to quantify the vegetation biomass by measuring the difference between near-infrared and red light. This index identifies vegetation reflection

and absorption for assessing vegetation density. These procedures resulted in a change analysis to identify and quantify how the salt marsh changed between two time periods. The results were then validated to confirm reliable outputs.

3.3. Unsupervised Classification

The unsupervised classification schemes used were K-means and IsoData. These schemes served as a pre-processing procedure to identify the effectiveness of using an unsupervised classification based solely on statistics. Each of these schemes focused on calculating statistics for each class. The IsoData unsupervised classification calculated class means that were distributed evenly throughout the image, while the remaining unselected pixels were grouped by their minimum value [57]. Through this repeated analysis, the means were recalculated, and the pixels were reclassified with respect to the new iteration of means [57]. This process continued until the number of pixels in each class changed by less than the selected pixel probability change threshold (0.8000) or the maximum number of iterations was reached (Figure 4).

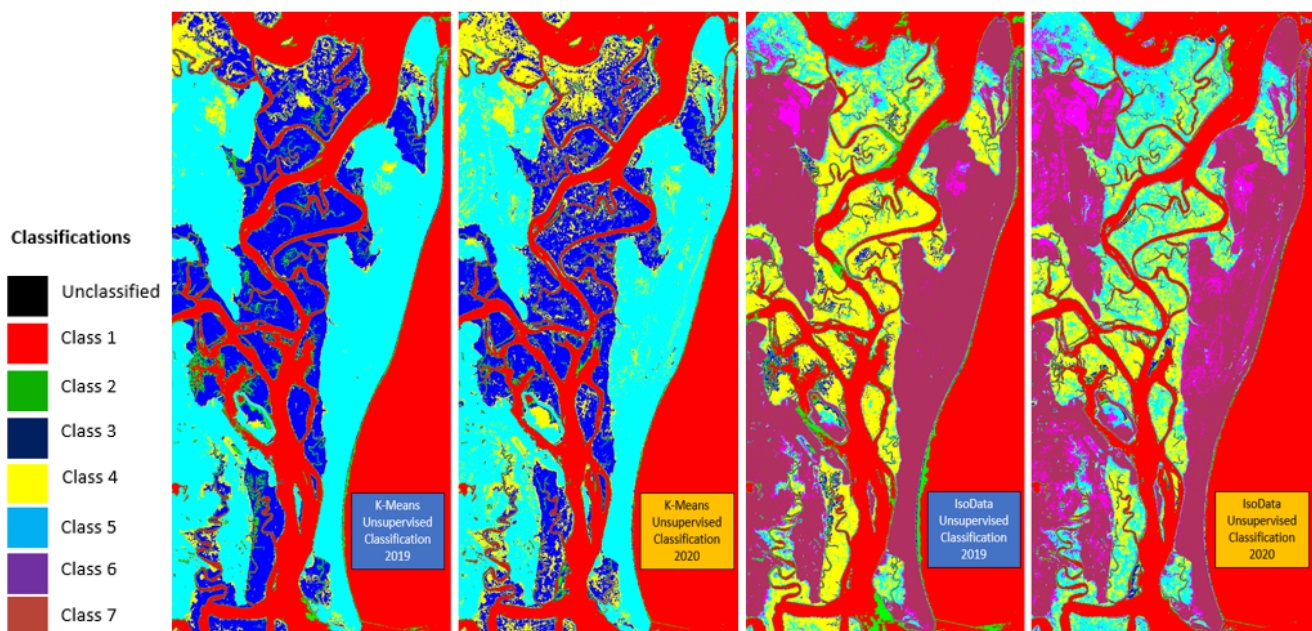


Figure 4. Unsupervised classification using IsoData and K-means at Cumberland Island NS from 2019 to 2020.

K-Means unsupervised classification calculated the original class means evenly throughout the image and then grouped the pixels to the nearest class using its minimum value calculated [57]. All pixels were classified to the nearest class using a probability threshold of 0.8000 (Figure 4). This process continued until the maximum number of classes was reached or the number of pixels in each class changed by less than the established threshold.

3.4. Supervised Classification

The supervised classification schemes clustered select pixels in the dataset on the basis of manual ROIs and field-based training data (Figure 5). The ROIs and training data were used to select each pixel that was representative of the determined features (water and marsh). The field-based training data incorporated 133 GPS points to identify salt marsh areas. These GPS points were added and matched to the pixel-based ROIs selected. Pixel-based ROIs were selected one at a time (1×1), or up to an area of 5×5 pixels on the raster layer was selected. Each selection or grouping of pixels was selected repeatedly to determine each class. The classification schemes used were maximum likelihood, minimum distance, Mahalanobis distance, and spectral angle mapper. The maximum likelihood

classification assumes that the statistical values for each class in each specified band are distributed evenly and calculates the probability that a given pixel belongs to the specified pre-determined class [57]. The probability threshold was a single value at 0.8000 for all classes. The data scale factor (default 255.00) was used as a division factor to convert integer scaled reflectance and radiance data into floating-point values. The no output rule image was applied.

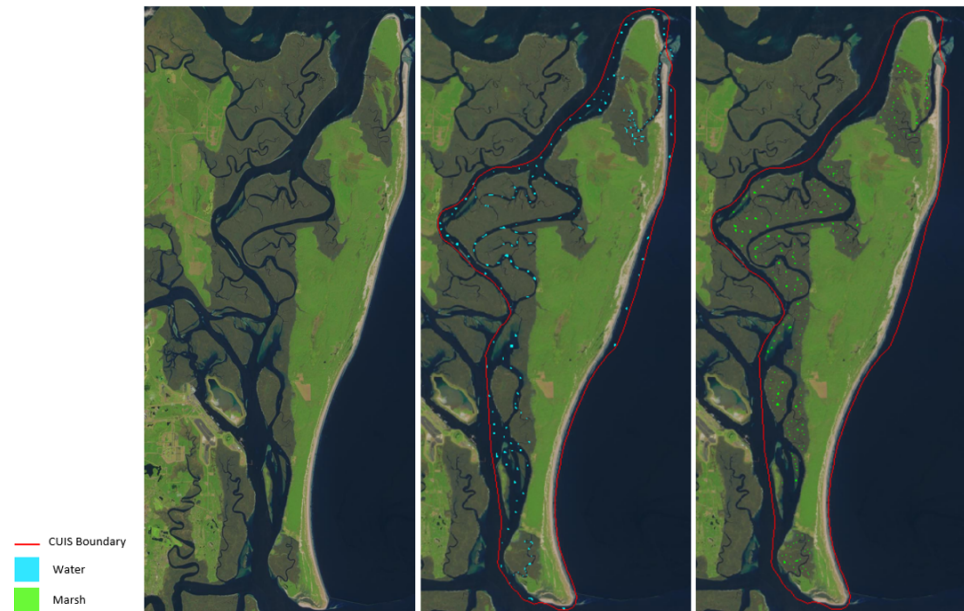


Figure 5. Manual ROIs and field-based training data of pixel selection to determine water and marsh areas.

3.5. Normalized Difference Vegetation Index (NDVI)

The NDVI was used to quantify the vegetation biomass to understand the vegetation density in the select sites. The NDVI is a ratio calculated between red light (RED) and near-infrared (NIR) values (formula below). The NDVI range is $-1 \leq X \leq 1$ (Figure 6). Negative values represent water, values close to zero ($-0.1 < X < 0.1$) represent bare soil/unconsolidated material, less positive values ($0.1 < X < 0.4$) represent sparse to intermediate vegetation, and values approaching 1 ($X \leq 1$) are categorized as dense vegetation [58–61].

$$\text{NDVI Formula: } \text{NDVI} = (\text{NIR} - \text{RED}) / (\text{NIR} + \text{RED})$$

Vegetation Classification and NDVI Index Values				
Different Land Areas	Water	Bare Soil/Unconsolidated Material	Sparse to Intermediate Vegetation	Dense Vegetation
NDVI Values	Negative Values	Values close to Zero	Low Positive Values	Values Approaching 1
NDVI Scale				
NDVI Values (X)	$X < 0$	$-0.1 < X < 0.1$	$0.1 < X < 0.4$	$X > 1$

Figure 6. NDVI vegetation classification and scale values.

3.6. Change Detection Analysis

The resulting change detection maps from the maximum likelihood classification scheme were used to identify increases/decreases in salt marsh area temporally. Band 3 (the green band) was selected to identify these changes by calculating the difference between the initial image and the final image during the specified period. Images were geometrically aligned with the same viewing geometry and coordinate system. To identify the increases and decreases in salt marsh area, the Otsu thresholding method was applied. This algorithm assumes that the image contains two classes of pixels and then calculates the optimum threshold separating the two classes [57]. The optimal threshold (or set of thresholds) is selected automatically; it is not based on differentiation but on the integration of the zeroth- to first-order cumulative moments of the gray-level histogram [62]. The Otsu thresholding algorithm is a nonparametric approach for automatic threshold identification and has been widely used in coastal wetland analysis [63–66].

3.7. Validation

The validation process was an evaluation of the processed data to confirm that the technique produced reliable outputs characterizing the spatial and temporal analysis of salt marshes. This approach incorporates validating a single classification (maximum likelihood) using the change detection analysis. The methods used to validate the results were (1) threshold output, (2) selection of ROIs, (3) identification of known open water sources, and (4) extraction of values to points. Each of the validation processes was operated through this classification to characterize the areas of under- and over-predictions for each site. These methods incorporated the manual ROIs, field-based training data, and probability threshold values to identify accuracy. The field-based training data consisted of 133 GPS points locating salt marsh areas. These points were used to validate that the areas classified as salt marsh were accurate.

To perform the threshold output validation technique, the established ROIs were processed under different probability thresholds to assess the maximum likelihood classification accuracy. The probability threshold value was used to identify the accuracy of the processed results under 0.80, 0.90, and 0.995. These threshold values were determined to ensure that the pixel was actually representative of the feature class. A probability threshold of 0.80 or better is stricter than a lower threshold value in allowing a pixel in a class. Each year was processed under all thresholds to select the pixels assigned to the class that had the highest probabilities according to the probability threshold set. If the highest probability is smaller than the specified threshold, the pixel remains unclassified.

ROI selection is a validation process of selecting 30% and 70% of the recorded ROIs to determine the difference in the output produced. The ROIs selected are random and do not follow a particular pattern. Each ROI was selected in both water and marsh areas.

The open water source validation process involves identifying how accurately the bodies of water are classified. This process is used to validate that all the areas mapped as water are in fact designated water sources. The purpose of using water body detection is to (1) identify how each classification scheme performed in identifying pixels of a different feature class, (2) how the water body results differ from salt marsh detection, (3) how the selection of water ROIs changes when they have neighboring salt marsh ROIs, and (4) whether the classification scheme can identify the changes occurring with the water bodies that ultimately impact the salt marshes.

The extraction of values to points was used to identify the accuracy of the classification scheme on the training data and ROIs created to identify the marsh areas and water sources. This process extracts the cell values of a raster on the basis of the set of point features and then records the values in the attribute table of an output feature class. The input raster is not resampled in the environment. Instead, the cell values are extracted from the input raster in its original resolution and spatial reference by projecting the input locations to the raster's reference from the values extracted.

4. Results

The results present the salt marsh change detection and NDVI outputs for the selected NPS sites (Cumberland Island NS, Fort Pulaski NM, and Canaveral NS) from 2016 to 2020. Areas designated as salt marsh increases/decreases feature the salt marsh area changes. They demonstrate how vulnerable salt marshes are along the southeastern US and highlight the effectiveness of this remote sensing technique to enhance coastal natural resource conservation.

4.1. Cumberland Island National Seashore

Cumberland Island NS was analyzed from 2019 to 2020, as this period exhibited no cloud cover over this specified region (Figure 7). The marsh areas, tributaries, channels, tidal inlets, and bodies of water were mapped effectively by the maximum likelihood classification scheme to capture changes occurring at this site.

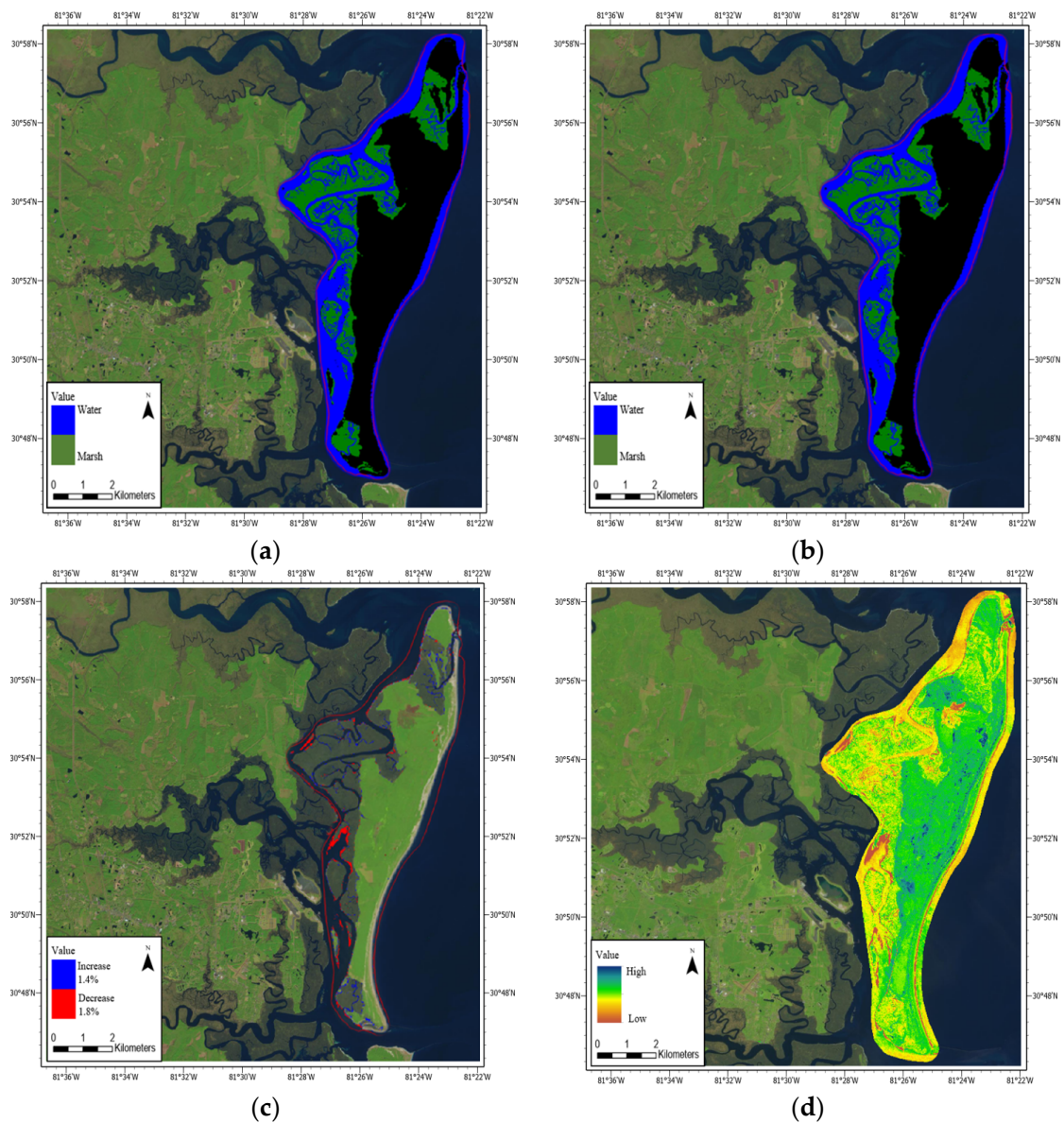


Figure 7. Maximum likelihood classification of Cumberland Island National Seashore from 2019 (a) to 2020 (b). (c) Change detection analysis of marsh land. (d) NDVI salt marsh assessment determining differential reflection of the vegetation density and relative growth using spectral reflectivity of solar radiation from 2019 to 2020.

The change detection analysis displayed shifts in tidal inlets and channels and along the coastline. There was a decrease of 1.8% in salt marsh, with a large portion of this decrease along channel inlets on the most westward areas of the site boundary (Figure 7). Areas detected as increases in salt marsh were identified in the western, northern, and southern regions of the site by 1.4% (Figure 7).

The NDVI results supported the maximum likelihood classification and change detection analysis. Increases and decreases in salt marsh were analogous in areas where water, bare soil, and sparse–intermediate vegetation were present. The NDVI values in the 2019 image ranged from -0.52 to 0.83 , and those in the 2020 image ranged from -0.48 to 0.78 (Figure 7). The vegetation index indicated bare soil/unconsolidated material around the entire site boundary. In the tidal inlets and channels, the NDVI values categorized the tidal inlets and channels as water and bare soil/unconsolidated material. Approaching the eastern region of the site from the west, the vegetation index indicated a transition from sparse–intermediate vegetation to dense vegetation. The areas categorized as marsh land ranged from bare soil/unconsolidated material to sparse–intermediate vegetation, while the most eastern region appeared to have small locations of dense vegetation.

4.2. Canaveral National Seashore

Canaveral NS was assessed from 2016 to 2017 through the maximum likelihood classification scheme (Figure 8). Through this scheme, some marshes were able to be identified; however, the water bodies were identified best. The black areas are areas that were not identified by the classification process. The change detection process was able to identify some of the classified salt marsh changes (Figure 9). Marsh areas in the southernmost region of the site had the largest decreases, while areas of marsh increase were represented in areas along the western and eastern boundaries of the site. The majority of changes identified were in the channels and tidal inlets; however, notable increases were present inland along the western site boundary.

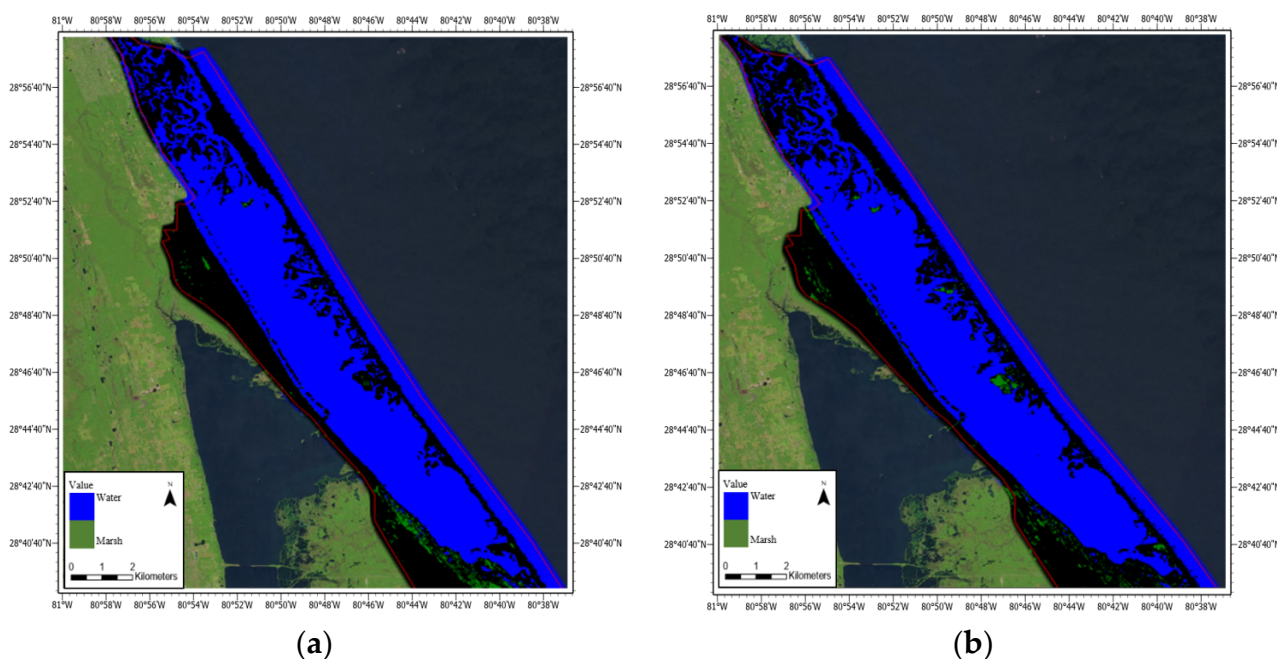


Figure 8. Supervised maximum likelihood classification of Canaveral National Seashore from 2016 to 2017. Image (a): 2016; image (b): 2017.

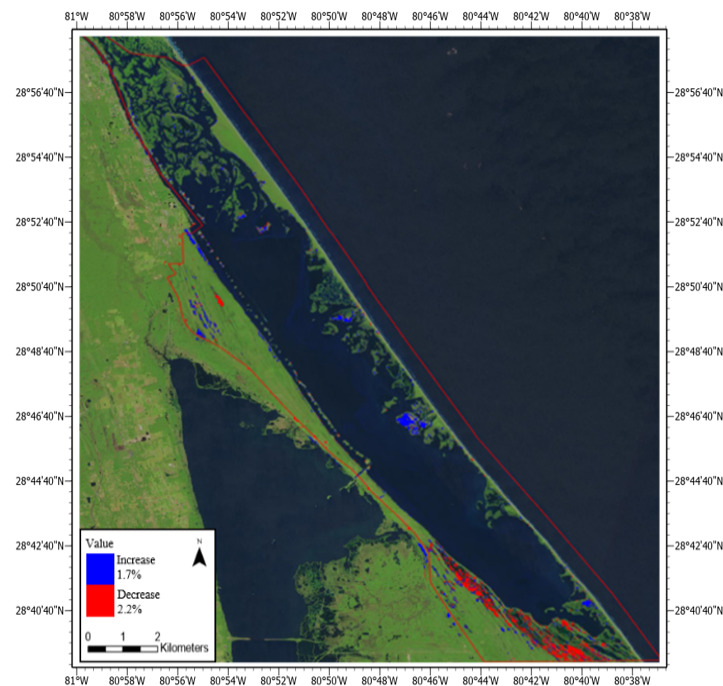


Figure 9. Canaveral National Seashore change detection analysis of marsh land from 2016 to 2017.

The NDVI results paired well with the change detection analysis (Figure 10). In this site, the vegetation index values for the 2016 image were -0.55 to 0.78 and -0.64 to 0.82 for 2017. The spectral signatures of the marshes along the eastern border of the site were considered to be water, bare soil/unconsolidated material, and sparse to intermediate vegetation.

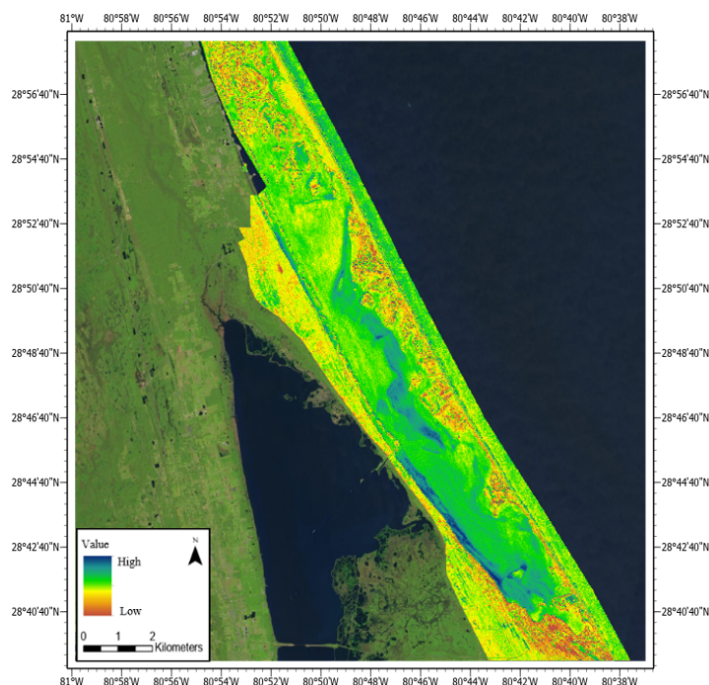


Figure 10. NDVI salt marsh assessment of Canaveral National Seashore displaying differential reflection of the vegetation density and relative growth using spectral reflectivity of solar radiation from 2016 to 2017.

4.3. Supervised Classification Accuracy

Supervised classification schemes, i.e., maximum likelihood, Mahalanobis distance, spectral angle mapper, and minimum distance, were used to assess the productivity of each method and its accuracy (Figure 11). The maximum likelihood produced the most accurate result, with 90% of the marsh pixels and 99% of the water pixels mapped accurately (Table 1).

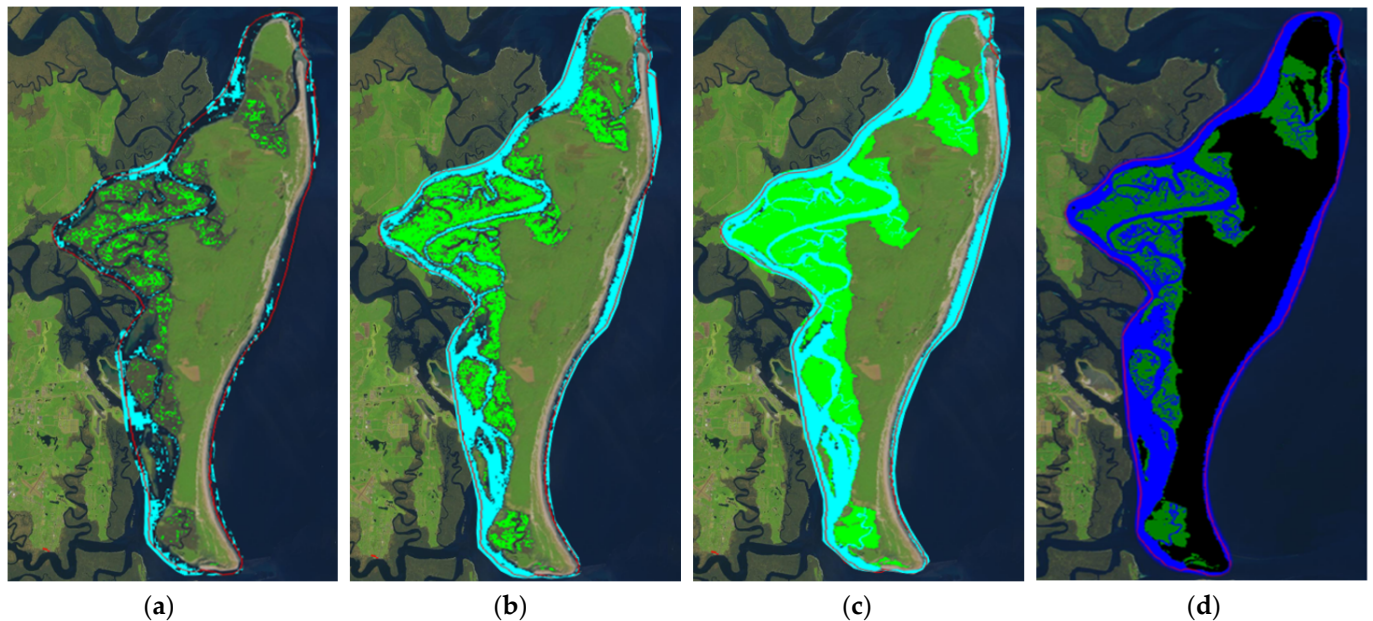


Figure 11. Supervised classification schemes: Mahalanobis distance (a), spectral angle mapper (b), minimum distance (c), and maximum likelihood classification (d).

Table 1. Supervised classification scheme accuracy of all ROIs inputted at Cumberland Island National Seashore.

Classifications	Supervised Classification Scheme Accuracy %			
	Marsh Pixels (270)	Marsh Accuracy %	Water Pixels (207)	Water Accuracy %
Maximum Likelihood	243	90%	207	99%
Minimum Distance	239	89%	197	95%
Spectral Angle Mapper	234	87%	168	81%
Mahalanobis Distance	62	23%	8	43%

4.4. Tidal Influence

Fort Pulaski NM highlights the importance of considering the tidal influence in diurnal environments (Figure 12). On 30 December 2016 and 21 October 2018, the tidal influence was 1.8–2.7 m. In conducting the supervised classification during this time, the results displayed the impact of seasonality on this environment. Due to the tidal stage, the marshes present were submerged, not removed.

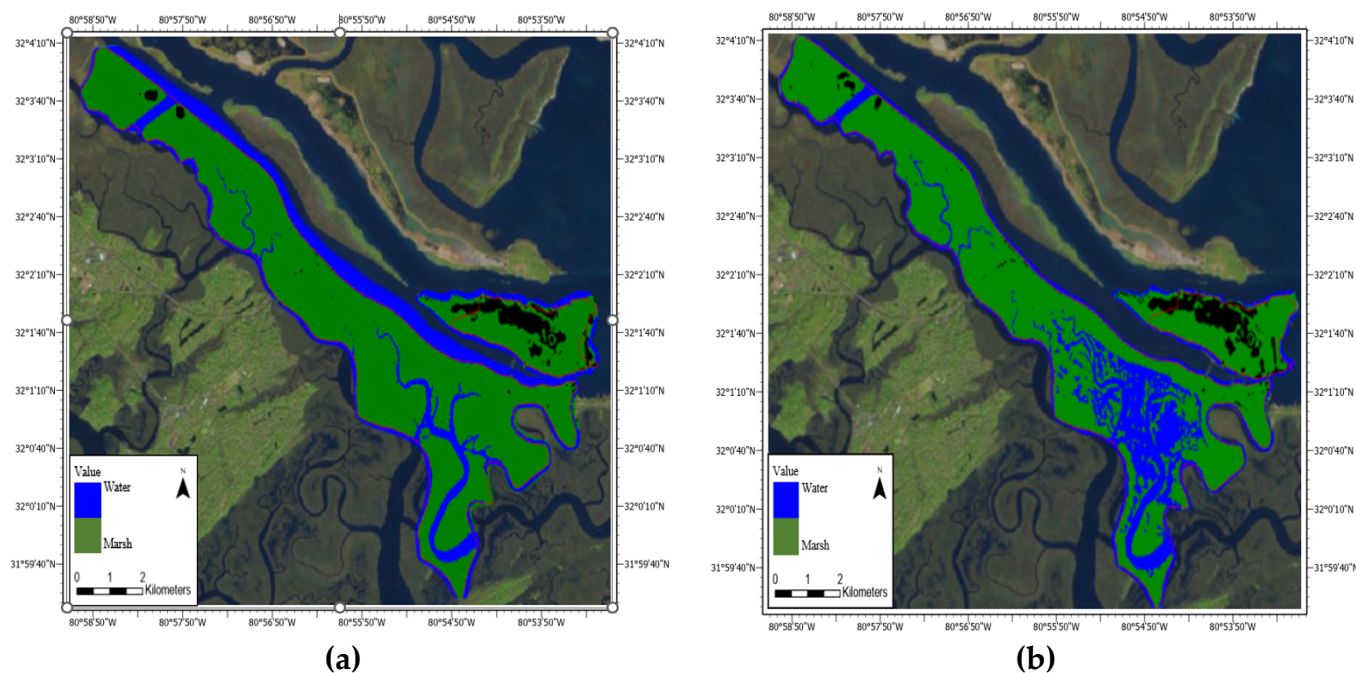


Figure 12. Supervised maximum classification of Fort Pulaski National Monument from 2016 to 2018. Image (a): 2016; image (b): 2018.

In this assessment, the change detection analysis was identifying areas where the marsh was submerged due to the tidal influence. These marsh areas were submerged in the tidal inlets and the southeast region of the site boundary. As these marsh environments are representative of dynamic processes, validating the maximum likelihood accuracy is a must (Table 2). The maximum likelihood classification validation results displayed the accuracy of this approach.

Table 2. Validation accuracy assessment from the maximum likelihood classification scheme for each site.

Validation Accuracy %			
Features	Input Points (ROIs)	Conferred Points	Accuracy %
Cumberland Island National Seashore			
Salt Marsh	270	242	90%
Water	207	205	99%
Canaveral National Seashore			
Salt Marsh	12	9	75%
Water	102	100	98%
Fort Pulaski National Monument			
Salt Marsh	240	226	94%
Water	71	70	99%

5. Discussion

In the southeastern US, salt marshes represent some of the most vulnerable wetlands. This research outlined the feasibility of using remote sensing-based classification methods for assessing salt marsh changes. Variations of this technique are widely known and have been applied to understand coastal vegetative changes; however, this methodology has not been utilized in this region, nor has it been assessed [67–69]. Before the supervised classification process was implemented, the unsupervised classification scheme was performed. The unsupervised classification produced seven classes that were determined from the statistical routine (i.e., clustering) on the basis of their shared spectral signatures. This is an important step because the classification categorizes unknown similarities and

differences in the data by grouping similar features. Although the identification of distinct features was determined, the algorithm generated multiple classes that represented a single feature (Figure 4). This is due to not having a training sample and/or an ROI to define each feature class accurately. Using the results of the unsupervised classification improved the supervised classification by selecting the necessary ROIs representative of the select features by the spectral signatures clustered. To enhance this automation process, the unsupervised classification can improve the number of classes determined, as too many classes can saturate the classification results, yielding inaccurate assumptions of the area analyzed. Improving the range of clustering from the spectral signatures of each pixel will provide better interpretation when training data are limited. The unsupervised classification serves its purpose when no training data exist, but it has to be coupled with a supervised classification scheme to ensure accurate results. According to these results, spectral angle mapper, minimum distance, and Mahalanobis distance were each selected to determine the best method from the supervised classification methods; however, the maximum likelihood classification results showed the most promise in accurately assessing marsh changes (Figure 11). Each NPS site was assessed through this scheme to determine whether this classification would produce an accurate interpretation of the environment. Each site was mapped appropriately through the manual input ROIs and field-based training data. The pixels selected captured similarly vegetated marsh areas in Canaveral NS and Cumberland Island NS (Figures 7 and 8). The channels and tidal inlets, where most of the changes occurred, also produced viable results. In selecting pixel-based ROIs, details matter, and in order to provide the most accurate interpretation, each individual pixel was selected randomly throughout the Sentinel-2 image. Pixels that neighbored another class or bordered a new feature class were not selected to prevent the over-estimation of another class feature. When all ROIs were combined, the maximum likelihood classification yielded the highest accuracy percentage (Table 1). Table 1 displays the number of marsh and water pixels that accurately represent these features. Subsequently, the input of all ROIs improved the performance of minimum distance and spectral angle mapper.

The NDVI provided a supportive source displaying the differential reflection of the vegetation biomass presence. This assessment supported the maximum likelihood classification and change detection analysis, displaying that the majority of the marsh areas in these sites were from bare/soil unconsolidated material to sparse-intermediate vegetation (Figures 7 and 10). In the areas where the results indicated salt marsh decreases, the NDVI values were less than zero, displaying no vegetation. By utilizing this vegetative index, spatial change relationships were captured, the distribution was quantified, and the accuracy of mapping was classified.

To further our interpretation of the salt marsh changes occurring, a change detection analysis was performed on each NPS site to determine the exact location of such changes. The results indicated that salt marshes were largely decreasing during the study period; however, there were areas of increase (Figures 7 and 9). Notably, the largest salt marsh decrease occurred in or around the channels, coastline, and tidal inlets. Studies have shown that the majority of the cases of diebacks, submergence, and/or removal have occurred within these geomorphological features [69–73]. As a result, these processes alter channelization, contributing to hydrologic and hydrogeological changes. In Fort Pulaski NM, we highlighted the influence of high/low tide in these environments (Figures 12 and 13). As a result of tidal influence, decreases in salt marshes are representative of salt marshes being submerged, not removed [72,73]. Hurricanes are common in the coastal southeastern US, causing rapid sea level rise and the submergence of salt marsh areas [74]. In understanding how rapidly these coastal areas change, it is important to note that in collecting data in these regions, the data must be tidally synced. In Figures 12 and 13, we demonstrate how data can be misinterpreted due to the data not being under the same tidal influence. Using this method to classify vegetative changes is efficient, but pre-data collection must be suitable to provide viable results in identifying areas of concern and areas where changes are occurring.

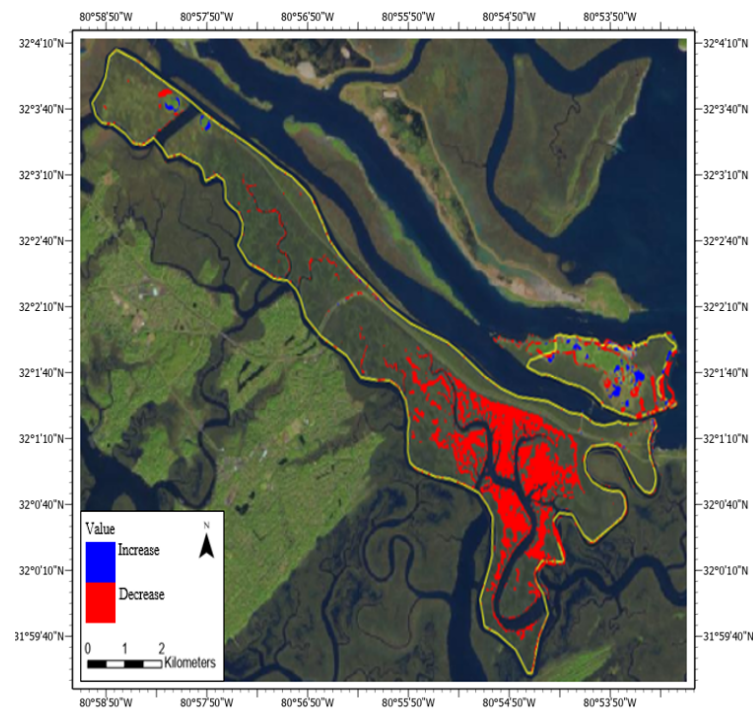


Figure 13. Fort Pulaski National Monument change detection analysis of marsh land from 2016 to 2018.

This study provides a detailed methodology that focuses on the establishment of a remote sensing-based procedure to classify salt marshes and detect changes in the marsh extent; however, some limitations are apparent. First, data availability and field-based data collection at each site would have increased the overall accuracy of the classification scheme used at Cumberland Island NS and Canaveral NS, as field-based training data were only applied to Fort Pulaski NM. Coupling field-based data to support this technique would have resulted in more precise results from the manually selected ROIs. Second, in completing this type of analysis, the spatial extent of the salt marshes must be considered. In areas where the extent of salt marshes is prominent, the maximum likelihood classification is efficient. Alternatively, if the areal extent of the salt marshes is relatively small, this procedure is not as effective in salt marsh monitoring. Third, the period in which data are collected must be considered. These datasets were collected because of their clarity due to a lack of cloud cover and the areal cover over the sites; however, due to differences in seasons, the amount of salt marsh present was impacted by diurnal variations. In the case of salt marsh studies, the tidal influence must be considered to alleviate misinterpretation. Fort Pulaski NM was not collected at approximately the same tidal level relative to a particular datum; however, even with this limitation, this method still highlighted areas of concern and showed how the salt marsh areas responded after being submerged. Lastly, the number of ROIs used when classifying each image must be taken into consideration. Overall, this classification scheme works best when there are more pixels selected in respect to its pixel value to provide a better interpretation. The more statistics collected for each band distributed spatially throughout the image, the higher probability that a given pixel or set of pixels belongs to a specific class feature. However, due to the classification scheme calculating each pixel, some results may yield an over- or underestimation of each feature class. This occurred while processing Canaveral NS, and therefore, the method was adjusted to capture an output that closely resembled the designated features. Fewer ROIs (12) were used to produce a more accurate result. Because Canaveral NS had a small areal extent of salt marsh presence, the maximum likelihood classification performed better with fewer ROIs selected. At this particular site, a higher number of ROIs produced an overestimation of salt marshes. Some of the pixels representative of salt marshes neighbored other features not representative of salt marshes in close proximity that yielded false results. Overall,

this classification scheme works best when there are more pixels selected in respect to its pixel value to provide a better interpretation. Even after considering these limitations, this multi-phased methodology was shown to be reliable in that it offers a high degree of performance and accuracy.

Studies have demonstrated that this method produces an overall accuracy ranging from 79% to over 88% [10,41,72,73]. In this study, we produced an overall accuracy ranging from 75% to 99% (Table 2). At each of the sites, the water bodies were mapped with 99% accuracy. In the marsh areas, the range was from 75% to 94% accuracy. The percentage of errors was likely due to the salt marshes' spatial extent, the inclusion of field-based data collection, and the variability of satellite imagery noise due to differences in the stage of tides. Due to the large spatial extent of the salt marshes at Fort Pulaski NM and Cumberland Island NS, the conferred points of the selected input ROIs yielded >90% accuracy. The maximum likelihood classification was able to better capture salt marsh features, as there were more pixels of identifiable marsh locations. Additionally, Fort Pulaski NM produced the most accurate results due to the combination of manual input ROIs and field-based data collection to yield more precise results.

6. Conclusions

Coastal salt marsh ecosystems are continually threatened by climatic effects and anthropogenic activity. As these ecosystems continue to experience these stressors and changes, analyzing changes in these environments will inevitably become more difficult due to their inaccessible locations and rapid transformation. The use of remote sensing-based techniques with high spatial resolutions offers a valuable tool to provide proper management and an understanding of these shifting ecosystems. Furthermore, coupling remote sensing-based techniques with field-based data collection can provide more accurate results in understanding the nature of the processes occurring in these environments.

In this study, we provided a detailed methodology that analyzed salt marshes in Cumberland Island NS, Fort Pulaski NM, and Canaveral NS. Through this approach, salt marshes were identified, changes in area were detected, and the NDVI was used to quantify the vegetation biomass to understand vegetation density changes. This study did not show a permanent loss, and changes in increases/decreases can be attributed to short-term changes between two periods. According to these results, repeatable assessments are warranted to identify long term trends. Through this process, we learned the critical state of these marsh environments as well as the value of applying these techniques. This advanced methodology has improved our understanding of the salt marsh changes occurring at these NPS sites while highlighting the disadvantages that exist in some scenarios.

This multi-phased technique furthers our understanding of the fundamental practices in analyzing coastal salt marshes through remote sensing-based approaches. As these detection techniques focused on salt marshes in this study, this application has the ability to be replicated under different environments and vegetation types. This developed framework enhances the reliability of change detection image processing due to the validated overall accuracy. As salt marshes continue to evolve, this approach offers the flexibility to capture ongoing changes. In a future study, deep learning, artificial neural networks, and support vector machine methods will have great potential for improving the classification of salt marshes.

To further characterize how vegetation is impacted by the effects of climate change, this study offers a monitoring tool that can be applied to improve coastal natural resource management. A field-based and remote sensing method is imperative in an uncertain climate and ever-changing ecomorphodynamic system, and utilizing this approach will ensure that salt marshes continue to serve as a pivotal resource in these aquatic environments.

Author Contributions: D.F.R.IV was the principal author of this manuscript and was responsible for the design, processing, interpretation, and writing of the manuscript. A.M.M. made significant contributions to the design, processing, interpretation, writing, and review of the manuscript. S.B., Y.D., L.J.D., F.J.Z., J.M. and M.D. helped with the design, interpretation, and review of the manuscript. All authors have read and agreed to the published version of the manuscript.

Funding: This research was funded by the National Park Service/Southeast Coast Inventory and Monitoring Network under task agreement P20AC00619.

Data Availability Statement: The data presented in this study are available upon request from the corresponding author.

Acknowledgments: The authors are grateful for Brian Gregory of the National Park Service Southeast Coast Inventory and Monitoring Network for his insights and review of this manuscript.

Conflicts of Interest: The authors declare no conflict of interest.

References

1. Barbier, E.B.; Hacker, S.D.; Kennedy, C.; Koch, E.W.; Stier, A.C.; Silliman, B.R. The value of estuarine and coastal ecosystem services. *Ecol. Monogr.* **2011**, *81*, 169–193. [CrossRef]
2. Crosby, S.C.; Sax, D.F.; Palmer, M.E.; Booth, H.S.; Deegan, L.A.; Bertness, M.D.; Leslie, H.M. Salt marsh persistence is threatened by predicted sea-level rise. *Estuar. Coast. Shelf Sci.* **2016**, *181*, 93–99. [CrossRef]
3. Simas, T.; Nunes, J.P.; Ferreira, J.G. Effects of global climate change on coastal salt marshes. *Ecol. Model.* **2001**, *139*, 1–15. [CrossRef]
4. Stagg, C.L.; Osland, M.J.; Moon, J.A.; Feher, L.C.; Laurenzano, C.; Lane, T.C.; Jones, W.R.; Hartley, S.B. Extreme precipitation and flooding contribute to sudden vegetation dieback in a coastal salt marsh. *Plants* **2021**, *10*, 1841. [CrossRef]
5. Alber, M.; Swenson, E.M.; Adamowicz, S.C.; Mendelssohn, I.A. Salt marsh dieback: An overview of recent events in the US. *Estuar. Coast. Shelf Sci.* **2008**, *80*, 1–11. [CrossRef]
6. Orson, R.; Panageotou, W.; Leatherman, S.P. Response of tidal salt marshes of the US Atlantic and Gulf coasts to rising sea levels. *J. Coast. Res.* **1985**, *1*, 29–37.
7. Schwarz, C.; van Rees, F.; Xie, D.; Kleinhans, M.G.; van Maanen, B. Salt marshes create more extensive channel networks than mangroves. *Nat. Commun.* **2022**, *13*, 2017. [CrossRef]
8. Mariotti, G.; Canestrelli, A. Long-term morphodynamics of muddy backbarrier basins: Fill in or empty out? *Water Resour. Res.* **2017**, *53*, 7029–7054. [CrossRef]
9. Guimond, J.; Tamborski, J. Salt marsh hydrogeology: A review. *Water* **2021**, *13*, 543. [CrossRef]
10. Byrd, K.B.; Kelly, M. Salt marsh vegetation response to edaphic and topographic changes from upland sedimentation in a Pacific estuary. *Wetlands* **2006**, *26*, 813–829. [CrossRef]
11. Craft, C.B.; Seneca, E.D.; Broome, S.W. Vertical accretion in microtidal regularly and irregularly flooded estuarine marshes. *Estuar. Coast. Shelf Sci.* **1993**, *37*, 371–386. [CrossRef]
12. Halpern, B.S.; Walbridge, S.; Selkoe, K.A.; Kappel, C.V.; Micheli, F.; d’Agrosa, C.; Bruno, J.F.; Casey, K.S.; Ebert, C.; Fox, H.E.; et al. A global map of human impact on marine ecosystems. *Science* **2008**, *319*, 948–952. [CrossRef] [PubMed]
13. Hartig, E.K.; Gornitz, V.; Kolker, A.; Mushacke, F.; Fallon, D. Anthropogenic and climate-change impacts on salt marshes of Jamaica Bay, New York City. *Wetlands* **2002**, *22*, 71–89. [CrossRef]
14. Kennish, M.J. Coastal salt marsh systems in the US: A review of anthropogenic impacts. *J. Coast. Res.* **2001**, *17*, 731–748.
15. South Atlantic Salt Marsh Initiative. Executive Summary: Marsh Forward—A Regional Plan for the Future of the South Atlantic Coast’s Million-Acre Salt Marsh Ecosystem. 2023. Available online: <https://www.marshforward.org> (accessed on 5 August 2023).
16. Crooks, S.; Herr, D.; Tamelander, J.; Laffoley, D.; Vandever, J. *Mitigating Climate Change through Restoration and Management of Coastal Wetlands and Near-Shore Marine Ecosystems: Challenges and Opportunities*; The World Bank: Washington, DC, USA, 2011.
17. Duarte, C.M.; Dennison, W.C.; Orth, R.J.; Carruthers, T.J. The charisma of coastal ecosystems: Addressing the imbalance. *Estuaries Coasts* **2008**, *31*, 233–238. [CrossRef]
18. Mcowen, C.J.; Weatherdon, L.V.; Van Bochove, J.W.; Sullivan, E.; Blyth, S.; Zockler, C.; Stanwell-Smith, D.; Kingston, N.; Martin, C.S.; Spalding, M.; et al. A global map of saltmarshes. *Biodivers. Data J.* **2017**, *5*, e11764. [CrossRef]
19. IPBES (Intergov. Sci. Policy Platf. Biodivers. Ecosyst. Serv.). The Assessment Report on Land Degradation and Restoration. Rep., IPBES, Bonn, Ger, 2018. Available online: <http://www.ipbes.net> (accessed on 18 June 2023).
20. Campbell, A.D.; Fatoyinbo, L.; Goldberg, L.; Lagomasino, D. Global hotspots of salt marsh change and carbon emissions. *Nature* **2022**, *612*, 701–706. [CrossRef]
21. Fretwell, S.; Wagner, A.; Lee, A. “A Million Acres of ‘Priceless’ Marshes Protect NC, SC, GA. Will They Perish in Rising Tides?” The News and Observer. 2021. Available online: <https://pulitzercenter.org/stories/million-acres-priceless-marshes-protect-nc-sc-ga-will-they-perish-rising-tides> (accessed on 18 June 2023).
22. Campbell, A.; Wang, Y. High spatial resolution remote sensing for salt marsh mapping and change analysis at Fire Island National Seashore. *Remote Sens.* **2019**, *11*, 1107. [CrossRef]

23. DiGiacomo, A.E.; Bird, C.N.; Pan, V.G.; Dobroski, K.; Atkins-Davis, C.; Johnston, D.W.; Ridge, J.T. Modeling salt marsh vegetation height using unoccupied aircraft systems and structure from motion. *Remote Sens.* **2020**, *12*, 2333. [[CrossRef](#)]
24. Roughgarden, J.; Running, S.W.; Matson, P.A. What does remote sensing do for ecology? *Ecology* **1991**, *72*, 1918–1922. [[CrossRef](#)]
25. Belluco, E.; Camuffo, M.; Ferrari, S.; Modenese, L.; Silvestri, S.; Marani, A.; Marani, M. Mapping salt-marsh vegetation by multispectral and hyperspectral remote sensing. *Remote Sens. Environ.* **2006**, *105*, 54–67. [[CrossRef](#)]
26. Silvestri, S.; Marani, M.; Marani, A. Hyperspectral remote sensing of salt marsh vegetation, morphology and soil topography. *Phys. Chem. Earth Parts A/B/C* **2003**, *28*, 15–25. [[CrossRef](#)]
27. Farris, A.S.; Defne, Z.; Ganju, N.K. Identifying salt marsh shorelines from remotely sensed elevation data and imagery. *Remote Sens.* **2019**, *11*, 1795. [[CrossRef](#)]
28. Zhang, M.; Ustin, S.L.; Rejmankova, E.; Sanderson, E.W. Monitoring Pacific coast salt marshes using remote sensing. *Ecol. Appl.* **1997**, *7*, 1039–1053. [[CrossRef](#)]
29. Fagherazzi, S.; Marani, M.; Blum, L.K. *The Ecogeomorphology of Tidal Marshes*; American Geophysical Union: Washington, DC, USA, 2004.
30. Silvestri, S.; Marani, M. Salt-marsh vegetation and morphology: Basic physiology, modelling and remote sensing observations. *Ecogeomorphology Tidal Marshes* **2004**, *59*, 5–25.
31. Day, J.W.; Christian, R.R.; Boesch, D.M.; Yáñez-Arancibia, A.; Morris, J.; Twilley, R.R.; Naylor, L.; Schaffner, L.; Stevenson, C. Consequences of climate change on the ecogeomorphology of coastal wetlands. *Estuaries Coasts* **2008**, *31*, 477–491. [[CrossRef](#)]
32. Scavia, D.; Field, J.C.; Boesch, D.F.; Buddemeier, R.W.; Burkett, V.; Cayan, D.R.; Fogarty, M.; Harwell, M.A.; Howarth, R.W.; Mason, C.; et al. Climate change impacts on US coastal and marine ecosystems. *Estuaries* **2002**, *25*, 149–164. [[CrossRef](#)]
33. Kirwan, M.L.; Mudd, S.M. Response of salt-marsh carbon accumulation to climate change. *Nature* **2012**, *489*, 550–553. [[CrossRef](#)]
34. Schuerch, M.; Vafeidis, A.; Slawig, T.; Temmerman, S. Modeling the influence of changing storm patterns on the ability of a salt marsh to keep pace with sea level rise. *J. Geophys. Res. Earth Surf.* **2013**, *118*, 84–96. [[CrossRef](#)]
35. Mwamba, M.J.; Torres, R. Rainfall effects on marsh sediment redistribution, North Inlet, South Carolina, USA. *Mar. Geol.* **2002**, *189*, 267–287. [[CrossRef](#)]
36. Valiela, I.; Teal, J.M.; Volkmann, S.; Shafer, D.; Carpenter, E.J. Nutrient and particulate fluxes in a salt marsh ecosystem: Tidal exchanges and inputs by precipitation and groundwater 1. *Limnol. Oceanogr.* **1978**, *23*, 798–812. [[CrossRef](#)]
37. Sanderson, E.W.; Ustin, S.L.; Foin, T.C. The influence of tidal channels on the distribution of salt marsh plant species in Petaluma Marsh, CA, USA. *Plant Ecol.* **2000**, *146*, 29–41. [[CrossRef](#)]
38. Tempest, J.A.; Harvey, G.L.; Spencer, K.L. Modified sediments and subsurface hydrology in natural and recreated salt marshes and implications for delivery of ecosystem services. *Hydrol. Process.* **2015**, *29*, 2346–2357. [[CrossRef](#)]
39. Hughes, A.L.; Wilson, A.M.; Morris, J.T. Hydrologic variability in a salt marsh: Assessing the links between drought and acute marsh dieback. *Estuar. Coast. Shelf Sci.* **2012**, *111*, 95–106. [[CrossRef](#)]
40. Wilson, A.M.; Evans, T.; Moore, W.; Schutte, C.A.; Joye, S.B.; Hughes, A.H.; Anderson, J.L. Groundwater controls ecological zonation of salt marsh macrophytes. *Ecology* **2015**, *96*, 840–849. [[CrossRef](#)] [[PubMed](#)]
41. Giri, C.; Ochieng, E.; Tieszen, L.L.; Zhu, Z.; Singh, A.; Loveland, T.; Masek, J.; Duke, N. Status and distribution of mangrove forests of the world using earth observation satellite data. *Glob. Ecol. Biogeogr.* **2011**, *20*, 154–159. [[CrossRef](#)]
42. Vo, Q.T.; Oppelt, N.; Leinenkugel, P.; Kuenzer, C. Remote sensing in mapping mangrove ecosystems—An object-based approach. *Remote Sens.* **2013**, *5*, 183–201. [[CrossRef](#)]
43. Berger, M.; Moreno, J.; Johannessen, J.A.; Levelt, P.F.; Hanssen, R.F. ESA's sentinel missions in support of Earth system science. *Remote Sens. Environ.* **2012**, *120*, 84–90. [[CrossRef](#)]
44. Dale, J.; Burnside, N.G.; Hill-Butler, C.; Berg, M.J.; Strong, C.J.; Burgess, H.M. The use of unmanned aerial vehicles to determine differences in vegetation cover: A tool for monitoring coastal wetland restoration schemes. *Remote Sens.* **2020**, *12*, 4022. [[CrossRef](#)]
45. Gorelick, N.; Hancher, M.; Dixon, M.; Ilyushchenko, S.; Thau, D.; Moore, R. Google Earth Engine: Planetary-scale geospatial analysis for everyone. *Remote Sens. Environ.* **2017**, *202*, 18–27. [[CrossRef](#)]
46. Campbell, A.D.; Wang, Y. Salt marsh monitoring along the mid-Atlantic coast by Google Earth Engine enabled time series. *PLoS ONE* **2020**, *15*, e0229605. [[CrossRef](#)] [[PubMed](#)]
47. Yeo, S.; Lafon, V.; Alard, D.; Curti, C.; Dehouck, A.; Benot, M.L. Classification and mapping of saltmarsh vegetation combining multispectral images with field data. *Estuar. Coast. Shelf Sci.* **2020**, *236*, 106643. [[CrossRef](#)]
48. McManamay, R.H. *Vegetation Mapping at Cumberland Island National Seashore*; Natural Resource Report NPS/SECN/NRR—2017/1511; National Park Service: Fort Collins, CO, USA, 2017.
49. McManamay, R.H.; Curtis, A.C.; Heath, S.C. *Vegetation Mapping at Fort Pulaski National Monument*; Natural Resource Report NPS/SECN/NRR—2013/718; National Park Service: Fort Collins, CO, USA, 2013.
50. Cotton, D.L.; Adams, B.P.; O'Hare, N.K.; Bernardes, S.; Jordan, T.R.; Madden, M. *Vegetation Mapping at Canaveral National Seashore: Photointerpretation Key and Final Vegetation Map*; Natural Resource Report NPS/SECN/NRR—2020/2084; National Park Service: Fort Collins, CO, USA, 2020.
51. Davey, C.A.; Redmond, K.T.; Simeral, D.B. *Weather and Climate Inventory, National Park Service, Southeast Coast Network*; Natural Resource Technical Report NPS/SECN/NRTR—2007/010; National Park Service: Fort Collins, CO, USA, 2007.
52. Pieschke, R.L. *U.S. Geological Survey Distribution of European Space Agency's Sentinel-2 Data: U.S. Geological Survey Fact Sheet 2017–3026*; U.S. Geological Survey: Sioux Falls, SD, USA, 2017; 2p. [[CrossRef](#)]

53. European Space Agency-Sentinel. 2022. Sentinel User Guides Product Type. Available online: <https://sentinels.copernicus.eu/web/sentinel/user-guides/sentinel-2-msi/product-types/level-1c> (accessed on 21 July 2023).
54. Aslan, A.; Rahman, A.F.; Warren, M.W.; Robeson, S.M. Mapping spatial distribution and biomass of coastal wetland vegetation in Indonesian Papua by combining active and passive remotely sensed data. *Remote Sens. Environ.* **2016**, *183*, 65–81. [[CrossRef](#)]
55. Giri, C.; Pengra, B.; Zhu, Z.; Singh, A.; Tieszen, L.L. Monitoring mangrove forest dynamics of the Sundarbans in Bangladesh and India using multi-temporal satellite data from 1973 to 2000. *Estuar. Coast. Shelf Sci.* **2007**, *73*, 91–100. [[CrossRef](#)]
56. Yagoub, M.M.; Kolan, G.R. Monitoring coastal zone land use and land cover changes of Abu Dhabi using remote sensing. *J. Indian Soc. Remote Sens.* **2006**, *34*, 57–68. [[CrossRef](#)]
57. NV5 Geospatial. 2022. ENVI Classification. Available online: <https://www.nv5geospatialsoftware.com/docs/Classification> (accessed on 21 July 2023).
58. Jones, H.G.; Vaughan, R.A. *Remote Sensing of Vegetation: Principles, Techniques, and Applications*; Oxford University Press: Oxford, UK, 2010.
59. Korchagina, I.A.; Goleva, O.G.; Savchenko, Y.Y.; Bozhikov, T.S. The use of geographic information systems for forest monitoring. In *Journal of Physics: Conference Series*; IOP Publishing: Bristol, UK, 2020; Volume 1515, p. 032077.
60. Huang, S.; Tang, L.; Hupy, J.P.; Wang, Y.; Shao, G. A commentary review on the use of normalized difference vegetation index (NDVI) in the era of popular remote sensing. *J. For. Res.* **2021**, *32*, 1–6. [[CrossRef](#)]
61. Nardin, W.; Taddia, Y.; Quitadamo, M.; Vona, I.; Corbau, C.; Franchi, G.; Staver, L.W.; Pellegrinelli, A. Seasonality and characterization mapping of restored tidal marsh by NDVI imageries coupling UAVs and multispectral camera. *Remote Sens.* **2021**, *13*, 4207. [[CrossRef](#)]
62. Otsu, N. A threshold selection method from gray-level histograms. *IEEE Trans. Syst. Man Cybermetrics* **1979**, *9*, 62–66. [[CrossRef](#)]
63. Xu, R.; Zhao, S.; Ke, Y. A simple phenology-based vegetation index for mapping invasive spartina alterniflora using Google Earth engine. *IEEE J. Sel. Top. Appl. Earth Obs. Remote Sens.* **2020**, *14*, 190–201. [[CrossRef](#)]
64. Jia, M.; Wang, Z.; Mao, D.; Ren, C.; Wang, C.; Wang, Y. Rapid, robust, and automated mapping of tidal flats in China using time series Sentinel-2 images and Google Earth Engine. *Remote Sens. Environ.* **2021**, *255*, 112285. [[CrossRef](#)]
65. Liu, Y.; Zhou, M.; Zhao, S.; Zhan, W.; Yang, K.; Li, M. Automated extraction of tidal creeks from airborne laser altimetry data. *J. Hydrol.* **2015**, *527*, 1006–1020. [[CrossRef](#)]
66. Kuleli, T.; Guneroglu, A.; Karsli, F.; Dihkan, M. Automatic detection of shoreline change on coastal Ramsar wetlands of Turkey. *Ocean. Eng.* **2021**, *38*, 1141–1149. [[CrossRef](#)]
67. Calzadilla Pérez, A.; Damen, M.C.J.; Geneletti, D.; Hobma, T.W. Monitoring a recent delta formation in a tropical coastal wetland using remote sensing and GIS. Case study: Guapo River delta, Laguna de Tacarigua, Venezuela. *Environ. Dev. Sustain.* **2002**, *4*, 201–219. [[CrossRef](#)]
68. Ogburn, M.B.; Alber, M. An investigation of salt marsh dieback in Georgia using field transplants. *Estuaries Coasts* **2006**, *29*, 54–62. [[CrossRef](#)]
69. Stagg, C.L.; Mendelssohn, I.A. Restoring ecological function to a submerged salt marsh. *Restor. Ecol.* **2010**, *18*, 10–17. [[CrossRef](#)]
70. Fagherazzi, S.; Kirwan, M.L.; Mudd, S.M.; Guntenspergen, G.R.; Temmerman, S.; D’Alpaos, A.; Van De Koppel, J.; Rybczyk, J.M.; Reyes, E.; Craft, C.; et al. Numerical models of salt marsh evolution: Ecological, geomorphic, and climatic factors. *Rev. Geophys.* **2012**, *50*. [[CrossRef](#)]
71. Fagherazzi, S.; Hannion, M.; D’Odorico, P. Geomorphic structure of tidal hydrodynamics in salt marsh creeks. *Water Resour. Res.* **2008**, *44*. [[CrossRef](#)]
72. Leung, L.Y.; Prasad, R. *Potential Impacts of Accelerated Climate Change: Third Annual Report of Work (No. PNNL-27452-Rev. 1)*; Pacific Northwest National Lab (PNNL): Richland, WA, USA, 2019.
73. Pham, T.D.; Xia, J.; Ha, N.T.; Bui, D.T.; Le, N.N.; Takeuchi, W. A review of remote sensing approaches for monitoring blue carbon ecosystems: Mangroves, seagrasses and salt marshes during 2010–2018. *Sensors* **2019**, *19*, 1933. [[CrossRef](#)]
74. Michener, W.K.; Blood, E.R.; Bildstein, K.L.; Brinson, M.M.; Gardner, L.R. Climate change, hurricanes and tropical storms, and rising sea level in coastal wetlands. *Ecol. Appl.* **1997**, *7*, 770–801. [[CrossRef](#)]

Disclaimer/Publisher’s Note: The statements, opinions and data contained in all publications are solely those of the individual author(s) and contributor(s) and not of MDPI and/or the editor(s). MDPI and/or the editor(s) disclaim responsibility for any injury to people or property resulting from any ideas, methods, instructions or products referred to in the content.